REPORT DOCUMENTATION PAGE

Form Approved
OMB No. 0704-0188

1. REPORT DATE (DD-MM-YYYY)	2. REPORT TYPE	3. DATES COVERED (From - To)
	Technical Papers	

4. TITLE AND SUBTITLE

Please see attached

5a. CONTRACT NUMBER

5b. GRANT NUMBER

5c. PROGRAM ELEMENT NUMBER

6. AUTHOR(S)

5d. PROJECT NUMBER
2308

5e. TASK NUMBER
M13C

5f. WORK UNIT NUMBER
346057

7. PERFORMING ORGANIZATION NAME(S) AND ADDRESS(ES)

Air Force Research Laboratory (AFMC)
AFRL/PRS
5 Pollux Drive
Edwards AFB CA 93524-7048

8. PERFORMING ORGANIZATION REPORT

9. SPONSORING / MONITORING AGENCY NAME(S) AND ADDRESS(ES)

Air Force Research Laboratory (AFMC)
AFRL/PRS
5 Pollux Drive
Edwards AFB CA 93524-7048

10. SPONSOR/MONITOR'S ACRONYM(S)

11. SPONSOR/MONITOR'S NUMBER(S)
Please see attached

12. DISTRIBUTION / AVAILABILITY STATEMENT

Approved for public release; distribution unlimited.

13. SUPPLEMENTARY NOTES

14. ABSTRACT

20030116 065

15. SUBJECT TERMS

16. SECURITY CLASSIFICATION OF:			17. LIMITATION OF ABSTRACT	18. NUMBER OF PAGES	19a. NAME OF RESPONSIBLE PERSON
a. REPORT	b. ABSTRACT	c. THIS PAGE			Leilani Richardson
Unclassified	Unclassified	Unclassified	A		19b. TELEPHONE NUMBER (include area code) (661) 275-5015

DTSV

FILE

Doug
To Talley
AFRL/VSA

MEMORANDUM FOR PRS (In-House Publication)

2305 M1 3C

FROM: PROI (STINFO)

25 Jan 2001

SUBJECT: Authorization for Release of Technical Information, Control Number: **AFRL-PR-ED-TP-2001-024**
Ronald W. Bates; David M. Golden, et al., "Experimental Study and Modeling of the Reaction H + O_2 + M -> HO_2 + M (M= Ar, N_2, H_2O) at Elevated Pressures and Temperatures Between 1050-1250 K"

Physical Chemistry and Chemical Physics Journal **(Statement A)**
(Deadline: None Listed)

Experimental study and modeling of the reaction $H + O_2 + M \rightarrow HO_2 + M$ (M= Ar, N_2, H_2O) at elevated pressures and temperatures between 1050-1250K

Ronald W. Bates*, David M. Golden, Ronald K. Hanson, and Craig T. Bowman

High Temperature Gasdynamics Laboratory, Department of Mechanical Engineering, Stanford University, Stanford, CA, USA 94305

Dedicated to Professor Jürgen Troe on his 60th birthday

The $H + O_2 + M \rightarrow HO_2 + M$ reaction was investigated at temperatures between 1050-1250 K and pressures from 7 to 152 bar behind reflected shock waves in gas mixtures of H_2, O_2, NO, and bath gases of Ar, N_2, and H_2O. Narrow linewidth laser absorption of NO_2 at 472.7 nm was used to measure quasi-steady NO_2 concentration plateaus in experiments designed to be sensitive only to the $H + O_2 + M \rightarrow HO_2 + M$ and the relatively well-known $H + NO_2 \rightarrow NO + OH$ and $H + O_2 \rightarrow OH + O$ reaction rates. The pressure dependence of the reaction was studied by measuring the fall-off of the reaction for M = Ar over a 10-152 bar pressure range. A simple modified Hindered-Gorin model of the transition state is used in an RRKM analysis of the results to facilitate comparisons of this work with measurements from other researchers at lower pressures. The RRKM calculations can also be described, using the simple functional form suggested by Troe, with the following: $k_\infty/cm^3molecule^{-1}s^{-1} = 4.7\times10^{-11}(T/300)^{0.2}$; $k_0(Ar)/cm^6molecule^{-2}s^{-1} = 2.0\times10^{-32}(T/300)^{-1.2}$; $k_0(N_2)/cm^6molecule^{-2}s^{-1} = 4.4\times10^{-32}(T/300)^{-1.3}$; $k_0(H_2O)/cm^6molecule^{-2}s^{-1} = 3.4\times10^{-31}(T/300)^{-1.0}$; $F_c = 0.7$ for Ar and N_2 and 0.8 for H_2O. Measured values of the reaction rate for M = Ar in the highest pressure experiments fall below both simple RRKM analysis and the more sophisticated treatment of Troe using an *ab initio* potential energy surface. Collision efficiencies of N_2 and H_2O relative to Ar at 1200K are 3.3 and 20 respectively.

Introduction

The reaction of hydrogen atoms with oxygen molecules to produce hydroperoxyl radicals (HO_2) in the presence of a "third body,"

$$H + O_2 + M \rightarrow HO_2 + M \qquad [1]$$

competes directly in combustion processes with the chain branching reaction that produces hydroxyl (OH) radicals and oxygen atoms. In the atmosphere, Reaction [1] plays a role in the conversion of H-atoms to reactive OH

* *Current Address: Air Force Research Laboratory, Aerophysics Branch, Space and Missile Propulsion Division, Propulsion Directorate, Edwards AFB, CA, USA 93524, Email: ronald.bates@edwards.af.mil*

radicals through the reaction of HO_2 with NO. Thus, the rate constants and the relative values of the efficiencies of various collision partners in Reaction [1] are of interest in modeling both combustion processes and atmospheric chemistry. Therefore this Reaction [1] has been the object of several experimental studies in bath gases such as nitrogen and argon and to lesser extent with water as the collision partner.

For reactions such as [1], which are unimolecular in the reverse direction, the rate constants are pressure as well as temperature dependent. Even when conditions do not encompass the low or high pressure limiting conditions, it is of interest to measure the rates at those limits in order to fully characterize the reaction for modeling purposes.

In an earlier study, Cobos, Hippler, and Troe[1] have measured the rate of Reaction[1] in Ar and N_2 at 300K and at pressures up to 200 bar. However, previous studies of this reaction at elevated temperatures have resulted in considerable variation of the results[2-19]. Figure 1 gives some idea of the scatter in the data for M = Ar. Due to a need to understand the behavior of this reaction in high-pressure combustion, we report in this paper measurements of the reaction rate for pressures up to 152 bar in Ar, N_2 and H_2O at temperatures between 1050-1250K. We compare our experimental results with an RRKM model and with a recent study of Troe[26].

Experiment and Data Reduction

The $H + O_2 + M \rightarrow HO_2 + M$ reaction was investigated at elevated temperatures and pressures using the Stanford High Pressure Shock Tube (HPST). Temperatures between 1050-1250 K and pressures from 7 to 152 bar were generated behind reflected shock waves in gas mixtures of H_2, O_2, NO and Ar. In separate experiments, N_2 and H_2O gases were added to study their effects as collision partners. The stainless steel driven section of the HPST is 5 cm in internal diameter and 5 m in length and was wrapped with thin copper sheets and heated using 13 separate heating zones to produce uniform temperature along its length. (Experiments were performed at three different wall temperatures, 97, 135 and 150 ºC. Uniformity of ± 3 ºC was maintained.) Seven piezoelectric transducers (PZT) installed at known intervals along the length of the shock tube were used to measure the spatial variation of the incident shock velocity and establish its value at the end wall. Incident shock attenuation in the heated HPST was typically 0.5-1.5% near the end-wall. Reflected shock conditions are calculated from the initial gas concentrations, temperature, pressure, incident shock velocity and attenuation using fundamental shock relations and employing a Peng-Robinson equation of state, which has been previously shown to accurately predict state variables for the conditions of the present study [21]. Using the measured absolute pressure time history from a piezoelectric transducer installed at the test location and simple isentropic relationships, the temperature time history was calculated to further correct the influence of attenuation on temperature.

Ashmore and Tyler[22] (1962) first observed the formation of a quasi-steady state for NO_2 in H_2/O_2 mixtures containing small amounts of NO for sufficiently high $[NO]/[O_2]$ ratios. Bromly et al.[13] (1995) used this observation to study the $H + O_2 + M \rightarrow HO_2 + M$ reaction [1] at atmospheric pressure in a flow reactor in the temperature range 700< T/K<825. They found that NO_2 reached a quasi-steady state plateau such that: $[NO_2]_{plateau} = k_1[M][O_2]/k_2$, where reaction [2] is the well-known process, $H + NO_2 \rightarrow NO + OH$.

Our approach is to extend this technique to higher temperature shock tube conditions. Through sensitivity analyses, experimental conditions were chosen so that the plateau levels in the NO_2 absorption are sensitive only to the well-known $H + O_2 \rightarrow OH + O$ reaction as well as to reaction [2] and reaction [1] itself. An example sensitivity analysis for a typical test condition is shown in Figure 2.

Using narrow linewidth laser absorption of NO_2 and measured NO_2 absorption coefficients, measured NO_2 absorption profiles can be quantitatively converted into NO_2 mole fraction profiles using Beer's Law. The absorption coefficient of NO_2 at 472.7nm has been accurately measured (± 3%) in our laboratory over a wide range of pressures and temperatures, including those reported in this work. No measurable pressure dependence has been found for elevated temperatures, which is expected based on the continuum nature of NO_2 absorption near 472.7nm Figure 3 shows the optical arrangement used to determine NO_2 absorption profiles. This figure also shows the arrangement of a rapid-tuning, narrow linewidth, 1.4 μm infrared (IR) diode laser absorption optical train used to determine pre-shock H_2O concentration in experiments with added water vapor. In the present experiments, the optical arrangement, laser diameter, and window inlet and exit apertures were adjusted to minimize spurious intensity fluctuations resulting from beam steering and scintillation due to flow perturbations in high pressure shock tube boundary layers. The sapphire windows were cut with the Z-axis normal to the laser propagation and were pressure-cycled in window mounts in order to minimize stress-induced birefringence effects while ensuring transmitted light from the shock tube reaches the detector. A typical data trace is shown in Figure 4.

The NO_2 mole fraction profiles were fit using a detailed reaction mechanism in which only the rate of Reaction [1] was adjusted. In this work, the chemical reaction mechanism consisted of the H-O-N subset of reactions from GRI-Mech v2.11 with an update made in the $O_2 + H_2O \rightarrow OH + HO_2$ reaction rate as recommended by Hippler et al.[23]. Also shown in Figure 4 is the fit obtained using this procedure, as well as lines indicating a ±5% variation in the fit value of the reaction rate for the $H + O_2 + Ar \rightarrow HO_2 + Ar$ reaction. Note that the sensitive portion of the fit occurs only in the NO_2 plateau region, as anticipated by the simple kinetic model introduced above. The disagreement in early formation times for NO_2 indicates some need for further improvement in reaction rates important during that time, but does not significantly influence the determination of the $H + O_2 + M \rightarrow HO_2 + M$ reaction rate.

Using the same experimental and data reduction techniques, we conducted a series of tests using argon as the collision partner to explore the pressure dependence of the $H + O_2 + Ar \rightarrow HO_2 + Ar$ reaction from 10-152 bar. Mixtures used were adjusted slightly to maintain the time of occurrence of the plateau region and to optimize the sensitivity of the plateau to the $H+O_2+M \rightarrow HO_2 +M$ reaction. At the highest pressures of the present study some sensitivity to the well-known $H + O_2 \rightarrow OH + O$ reaction is observed. The data from these experiments are shown in Figure 5.

To study N_2 and H_2O as collision partners, test gas mixtures were adjusted to maintain sensitivity to Reaction [1] while portions of the argon bath gas were replaced with the new collision partner (for N_2, this is about 66%, for H_2O this is typically 3-7%). For experiments involving H_2O, Ar gas was bubbled through an adiabatic saturator and then subsequently mixed with the test gas mixture prior to being introduced to the heated HPST driven section. Pre-shock H_2O mole fractions were determined by fitting the 1.4 μm IR diode laser scans with a 4-line synthetic spectra model developed at Stanford [24]. Figure 6 shows data for all three collision partners as a function of pressure at 1200K. argon. All data are tabulated in Table 1. Uncertainty analyses weighting the uncertainties in chemical reaction rates for interfering reactions, temperature, absorption coefficient, and experimental noise indicate absolute accuracy of the lowest pressure data points as ±18% increasing to ±30% at the highest pressures .

Modeling and Discussion

We have used a modified Hindered-Gorin[25] model to rationalize the results of this work and the earlier work of Cobos, Hippler and Troe[1]. In the Hindered-Gorin model, that often is used to model bond breaking (or bond making) reactions, the transition state is represented by the two separate species, with the rotations along the axes perpendicular to the breaking bond restricted in the sense of being allowed to rotate in only some fraction of the 4π steradians of free space, thus increasing the rotational energy level spacing. This is achieved computationally by diminishing the moments of inertia, typically by $((100-\eta)/100)^{\frac{1}{2}}$ for each moment. The parameter η is referred to as the percent hindrance and has been found to exceed 90% in most cases.

For the transition state in reaction [1], where there are only two internal degrees of freedom, one of which is essentially the vibration in O_2, we have treated the H· · · O=O bend as a one-dimensional hindered rotor of the oxygen molecule. The moment of inertia of this rotation was lowered from the simple geometric value to match the data at 300K in Cobos, Hippler and Troe. The same value was used at 1200K. The collision efficiency that matches the Cobos, Hippler and Troe data at 300K was allowed to vary with temperature according to the simple formula of Troe[1]. The transition state geometry was obtained by stretching the H-O bond by a factor of $(6\Delta H/RT)^{1/6}$. Details of the transition state properties are given in Table 2. The collision efficiencies determined from the simple formula of Troe are tabulated in Table 3.

Troe[25] has recently proposed an analytical function to fit data for this reaction. We have also applied this function to the present data. We are unable to distinguish between the Troe function[25] and our RRKM results, neither of which fits the highest pressure results in argon. Figure 6 shows our experimental results for Ar in comparison with our RRKM calculations, Troe's suggestions and the Troe simple equation.. Figure 7 shows our RRKM results in comparison to the data for Ar, N_2, and H_2O.

Our RRKM calculations may be fit using the functional form suggested by Troe[25],

$k/ k_\infty = [x/(1+x)]F(x)$

$\log[F(x)] =[\{1+[\log(k_0/k_\infty)]^2\}^{-1}] \times \log[F_c]$

with the following parameters.

$k_\infty/cm^3molecule^{-1}s^{-1} = 4.7\times10^{-11}(T/300)^{0.2}$

$k_0(Ar)/cm^6molecule^{-2}s^{-1} = 2.0\times10^{-32}(T/300)^{-1.2}$

$k_0(N_2)/cm^6molecule^{-2}s^{-1} = 4.4\times10^{-32}(T/300)^{-1.3}$

$k_0(H_2O)/cm^6molecule^{-2}s^{-1} = 3.4\times10^{-31}(T/300)^{-1.0}$

$F_c = 0.7$ for Ar and N_2 and 0.8 for H_2O

This fit is also shown in Figure 6.

While the collision efficiencies are contained in the rate constants above, their relative values are of some interest and are given in Table 3.

Conclusions

The $H + O_2 + M \rightarrow HO_2 + M$ reaction [1] was investigated at temperatures between 1050-1250 K and pressures from 7 to 152 bar behind reflected shock waves in gas mixtures of H_2, O_2, NO, and bath gases of Ar, N_2, and H_2O carefully selected to achieve NO_2 plateaus sensitive to reaction [1], reaction [2], and $H + O_2 \rightarrow OH + O$ reaction. Narrow linewidth laser absorption of NO_2 at 472.7 nm was used to measure the quasi-steady NO_2 concentration plateaus. The pressure dependence of the reaction was studied by measuring the fall-off of the reaction for M = Ar over a 10-150 bar pressure range. We have determined the rate coefficient for reaction [1] with Ar, N_2 and H_2O as collision partners. The collision efficiencies in Table 3 can be used in chemical modeling in the format accepted by CHEMKIN.

The function suggested by Troe can be used either with the parameters suggested by him or those in this paper for Ar and N_2 as bath gases. Neither will fit the highest pressure Ar data. Future work will be undertaken to resolve

this discrepancy. Troe does not give sufficient parameters for use of his formalism when water is the bath gas. We have cast RRKM calculations for water as the bath gas in the same format as argon and nitrogen.

Water is a significantly more efficient collision partner than either Ar or N_2. This is expected based on its polar nature, but may also be due to chemical interactions.

Acknowledgements

We gratefully acknowledge the assistance of John Herbon, David Horning, Dr. Venu Nagali, and Dr. David Davidson for assistance in the laboratory during these experiments. One of the authors, (RWB), was supported by the USAF Palace Knights Program during this work. This work was supported by the Department of Energy, Office of Basic Energy Sciences.

Fig. 1 Reaction rate data available for $H + O_2 + Ar \rightarrow HO_2 + Ar$ from previous studies. (X) Ashman and Haynes[18], (*) Mueller et al.[19], (+) Michael et al.[27], (•) Pirraglia et al.[2], (•) Skinner and Ringrose,[3] (▽) Pamidimukkula and Skinner[4], (•) Chiang and Skinner[5], (•) Gutman et al.[6], (•) Davidson et al.[17], (•) Getzinger and Schott[9], (•) Getzinger and Blair[7].

Fig. 2 NO_2 plateau sensitivity for a typical M = Ar experiment.

Fig.3 Experiment setup for laser-based absorption measurements of NO_2 (472.7 nm) and H_2O (1405 nm) in the HPST experiments.

Fig. 4 Typical NO_2 absorption and mole fraction profile in an M = Ar experiment. The experimental conditions are identical to those in Figure 2. The full line represents a fit to the data using the procedure described in the text. The dashed lines show variation of k_1 by ±5%

Fig. 5 Measured $H + O_2 + Ar \rightarrow HO_2 + Ar$ reaction rate. For comparison purposes, k_0 from the RRKM fit and the GRI-Mech v3.0 mechanism are shown with the recent measurements of Ashman and Haynes[18], Mueller et al.[19], and Michael et al.[27].

Fig. 6 Comparison of measured M = Ar reaction rate at 1200K with the simple Hindered-Gorin RRKM model[25], the more sophisticated model of Troe[26], and a simplified functional expression using the form suggested by Troe[26].

Fig. 7 Measured reaction rate at 1200K for M = Ar, N_2, H_2O shown in comparison to the simple Hindered-Gorin RRKM model.

Table 1 Measured reaction rate coefficients for Ar, N_2, H_2O.

Table 2 Normal and Transition State Properties of HO_2 used in the simple Hindered-Gorin RRKM Analysis.

Table 3 Collision Efficiencies determined from simple Hindered-Gorin RRKM Analysis.

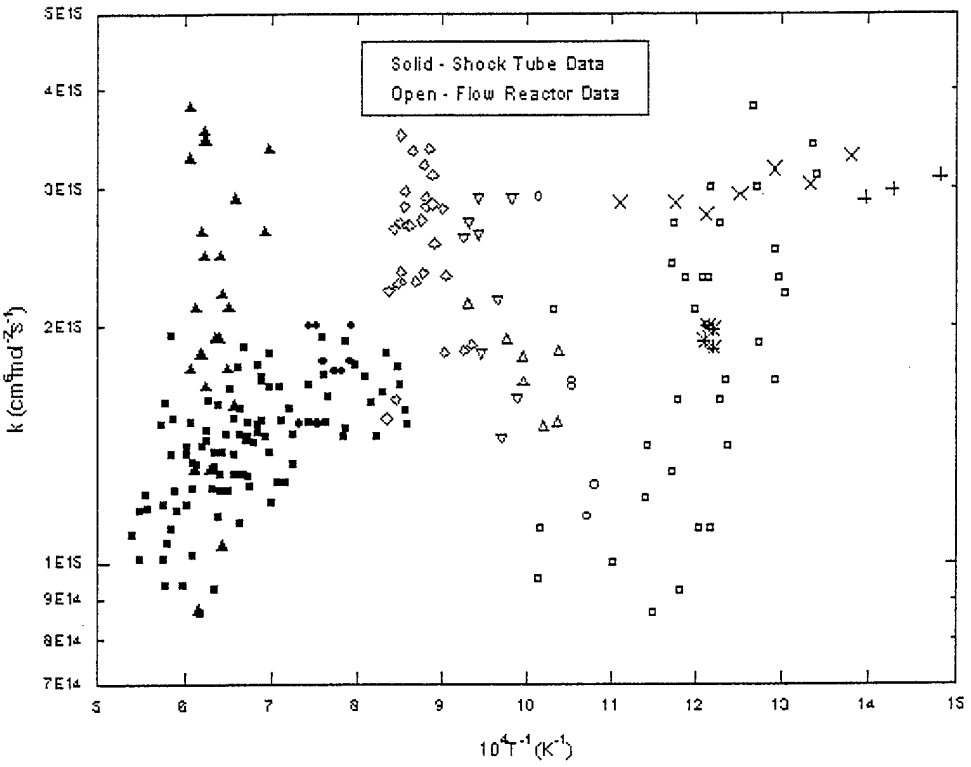
Solid - Shock Tube Data
Open - Flow Reactor Data
5E15
4E15
3E15
2E15
1E15
9E14
8E14
7E14
k (cm⁶md⁻²s⁻¹)
5
6
7
8
9
10
11
12
13
14
15
10⁴T⁻¹(K⁻¹)

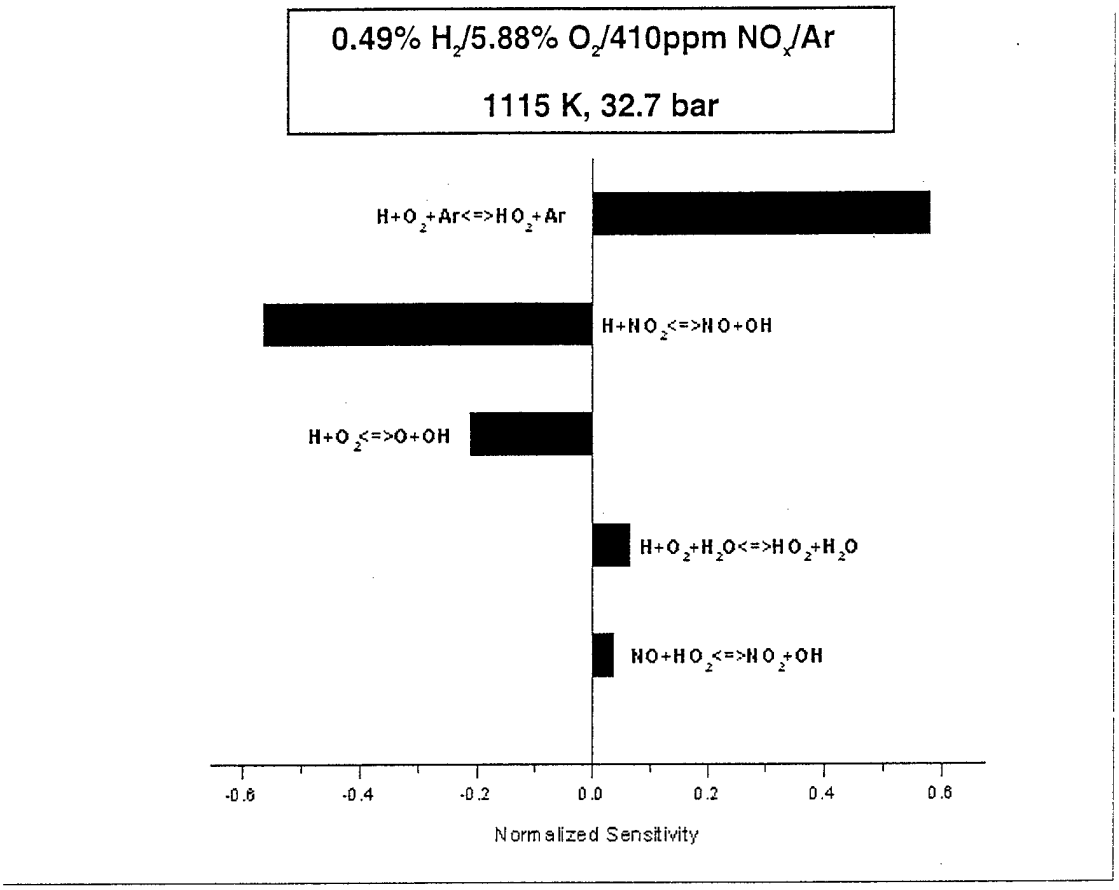
0.49% H2/5.88% O2/410ppm NOx/Ar
1115 K, 32.7 bar
H+O2+Ar<=>HO2+Ar
H+NO2<=>NO+OH
H+O2<=>O+OH
H+O2+H2O<=>HO2+H2O
NO+HO2<=>NO2+OH
-0.6
-0.4
-0.2
0.0
0.2
0.4
0.6
Normalized Sensitivity

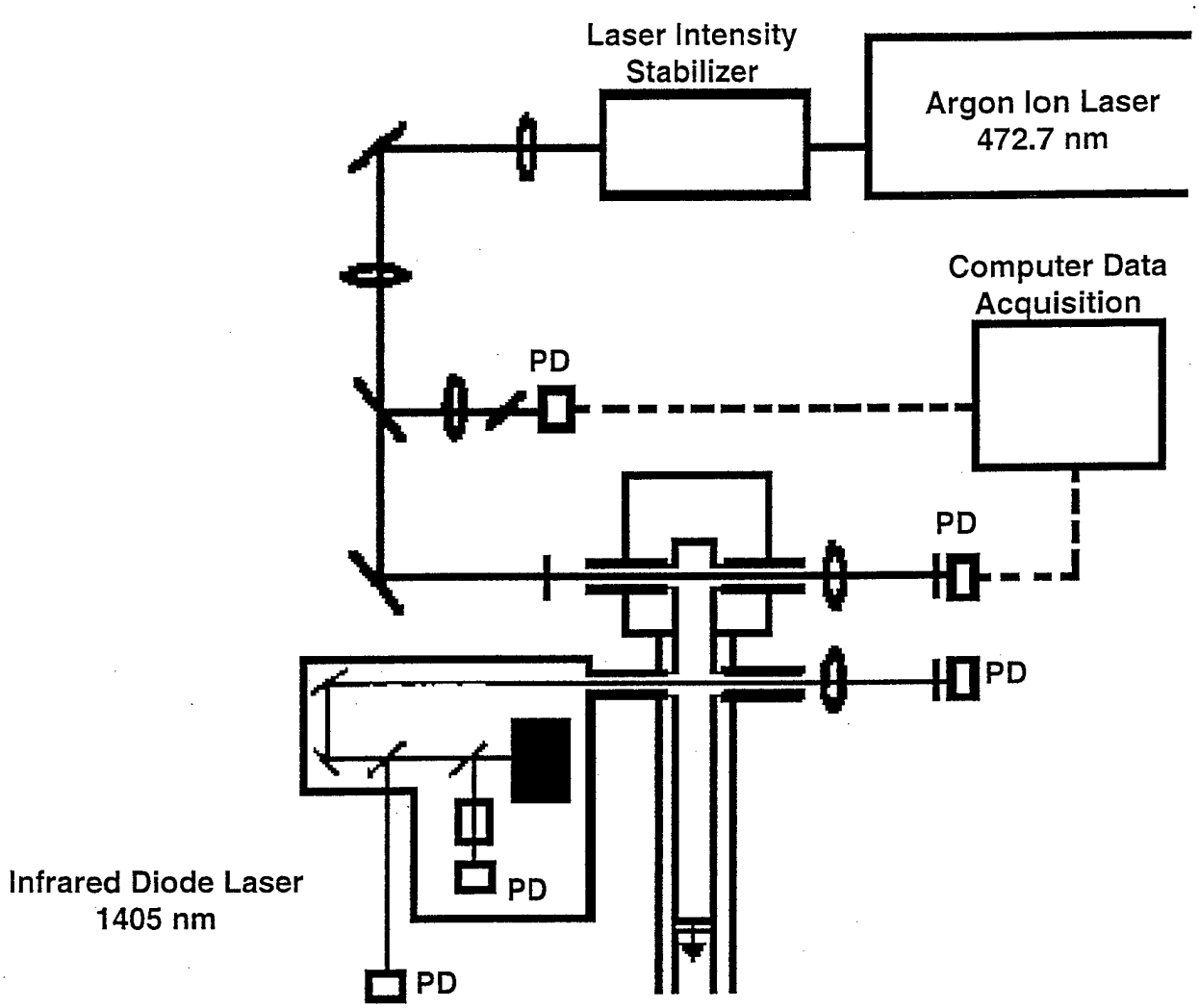
Laser Intensity
Stabilizer
Argon Ion Laser
472.7 nm
Computer Data
Acquisition
PD
PD
PD
PD
Infrared Diode Laser
1405 nm
PD

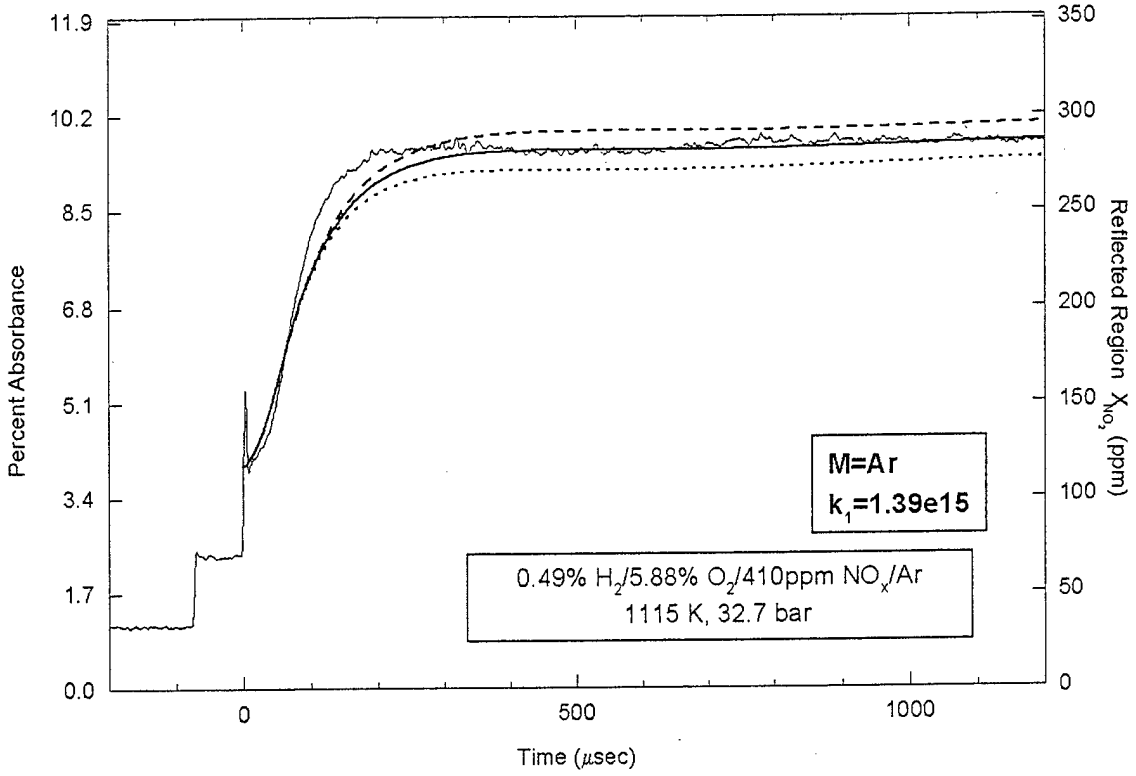
11.9
10.2
8.5
6.8
5.1
3.4
1.7
0.0
Percent Absorbance
0
500
1000
Time (μsec)
350
300
250
200
150
100
50
0
Reflected Region X_{NO_2} (ppm)
M=Ar
k_1=1.39e15
0.49% H_2/5.88% O_2/410ppm NO_x/Ar
1115 K, 32.7 bar

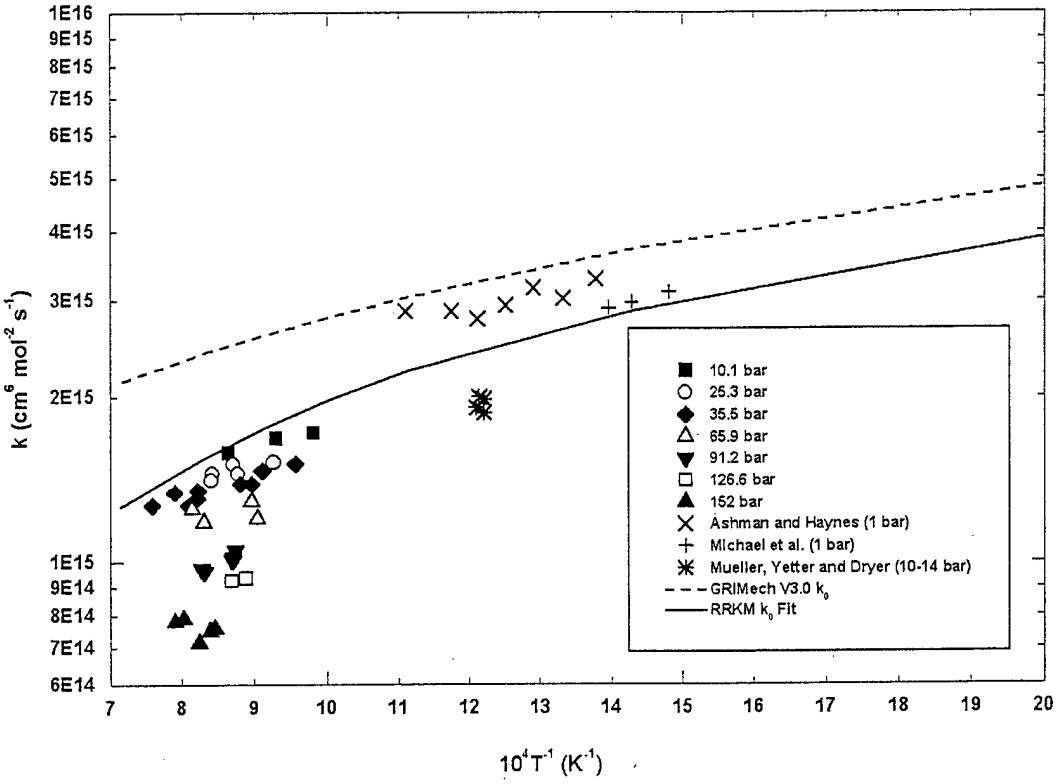
1E16
9E15
8E15
7E15
6E15
5E15
4E15
3E15
2E15
1E15
9E14
8E14
7E14
6E14
k (cm^6 mol^-2 s^-1)
7
8
9
10
11
12
13
14
15
16
17
18
19
20
10^4 T^-1 (K^-1)
10.1 bar
25.3 bar
35.5 bar
65.9 bar
91.2 bar
126.6 bar
152 bar
Ashman and Haynes (1 bar)
Michael et al. (1 bar)
Mueller, Yetter and Dryer (10-14 bar)
GRIMech V3.0 k0
RRKM k0 Fit

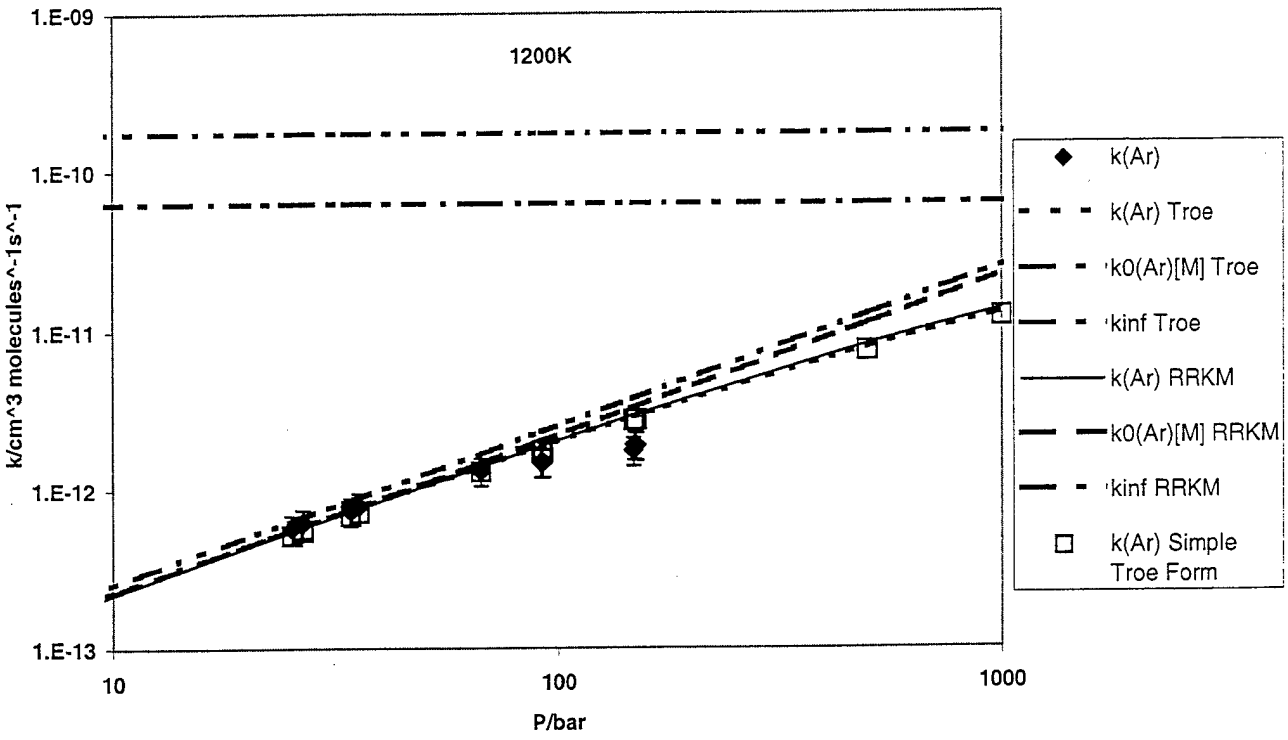
1200K
1.E-09
1.E-10
1.E-11
1.E-12
1.E-13
k/cm^3 molecules^-1s^-1
10
100
1000
P/bar
k(Ar)
k(Ar) Troe
k0(Ar)[M] Troe
kinf Troe
k(Ar) RRKM
k0(Ar)[M] RRKM
kinf RRKM
k(Ar) Simple Troe Form

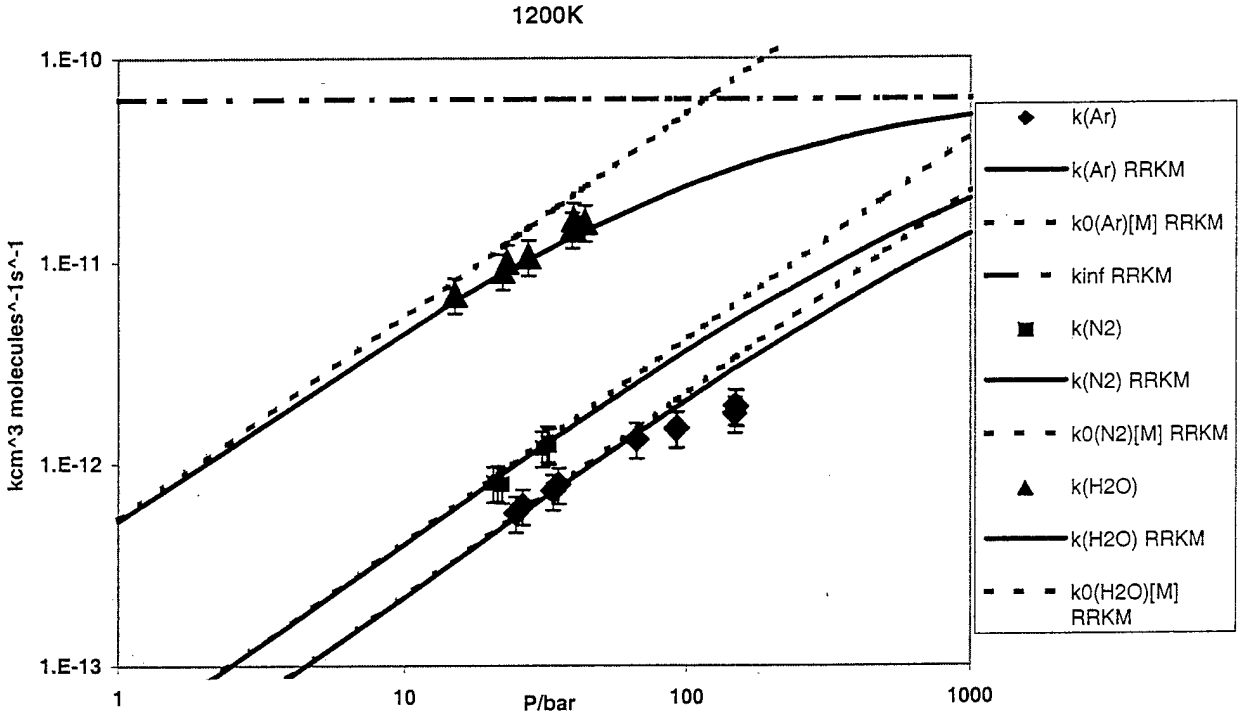
1200K
1.E-10
1.E-11
1.E-12
1.E-13
kcm^3 molecules^-1s^-1
1
10
100
1000
P/bar
k(Ar)
k(Ar) RRKM
k0(Ar)[M] RRKM
kinf RRKM
k(N2)
k(N2) RRKM
k0(N2)[M] RRKM
k(H2O)
k(H2O) RRKM
k0(H2O)[M] RRKM

Table 1

M = Ar				
Temperature (K)	Pressure (bar)	10^4/T (K^{-1})	M (molecules cm^{-3})	k (cm^3 $molecules^{-1}$ s^{-1})
1156.0	11.24	8.65	7.040E+19	3.06E-13
1074.8	11.32	9.30	7.627E+19	3.53E-13
1018.6	10.07	9.82	7.161E+19	3.39E-13
1138.8	23.43	8.78	1.490E+20	5.95E-13
1188.4	25.34	8.42	1.544E+20	6.00E-13
1078.3	24.15	9.27	1.622E+20	6.82E-13
1185.7	26.79	8.43	1.636E+20	6.52E-13
1146.9	24.60	8.72	1.554E+20	6.49E-13
1234.6	40.38	8.10	2.369E+20	8.30E-13
1216.0	34.19	8.22	2.036E+20	7.35E-13
1045.0	26.37	9.57	1.828E+20	7.60E-13
1134.0	33.20	8.82	2.121E+20	8.15E-13
1215.0	35.68	8.23	2.127E+20	7.92E-13
1115.0	32.75	8.97	2.127E+20	8.16E-13
1264.2	38.54	7.91	2.208E+20	8.14E-13
1316.8	38.68	7.59	2.127E+20	7.45E-13
1097.1	31.67	9.11	2.091E+20	8.47E-13
1105.7	67.47	9.04	4.420E+20	1.46E-12
1227.1	73.65	8.15	4.347E+20	1.50E-12
1115.0	66.21	8.97	4.301E+20	1.53E-12
1202.9	67.14	8.31	4.042E+20	1.32E-12
1207.9	92.56	8.28	5.550E+20	1.49E-12
1148.1	92.18	8.71	5.815E+20	1.61E-12
1144.6	91.39	8.74	5.782E+20	1.67E-12
1202.0	93.50	8.32	5.634E+20	1.50E-12
1149.0	92.62	8.70	5.838E+20	1.63E-12
1146.5	99.00	8.72	6.254E+20	1.76E-12
1124.7	127.06	8.89	8.182E+20	2.11E-12
1150.0	130.34	8.70	8.209E+20	2.09E-12
1212.6	150.09	8.25	8.965E+20	1.77E-12
1191.0	152.22	8.40	9.256E+20	1.91E-12
1181.9	150.73	8.46	9.237E+20	1.93E-12
1264.1	146.93	7.91	8.418E+20	1.81E-12
1245.3	148.14	8.03	8.616E+20	1.87E-12
M=N_2				
Temperature (K)	Pressure (bar)	10^4/T (K^{-1})	M (molecules cm^{-3})	k (cm^3 $molecules^{-1}$ s^{-1})
1119.3	8.15	8.93	5.271E+19	3.66E-13
1135.7	7.33	8.81	4.672E+19	3.18E-13
1191.6	21.67	8.39	1.317E+20	8.13E-13
1180.0	20.94	8.47	1.285E+20	8.05E-13
1222.0	22.58	8.18	1.338E+20	7.96E-13
1189.3	31.30	8.41	1.906E+20	1.20E-12
1199.5	33.04	8.34	1.995E+20	1.24E-12
1194.5	32.74	8.37	1.985E+20	1.27E-12
M=H_2O				
Temperature (K)	Pressure (bar)	10^4/T (K^{-1})	M (molecules cm^{-3})	k (cm^3 $molecules^{-1}$ s^{-1})
1184.2	15.20	8.44	9.296E+19	6.92E-12
1262.0	27.97	7.92	1.605E+20	1.07E-11
1151.2	23.45	8.69	1.475E+20	1.01E-11
1217.7	22.65	8.21	1.347E+20	9.12E-12
1109.0	36.14	9.02	2.360E+20	1.49E-11
1167.0	39.82	8.57	2.471E+20	1.46E-11
1082.0	34.55	9.24	2.313E+20	1.52E-11
1178.0	40.37	8.49	2.482E+20	1.63E-11
1100.0	35.32	9.09	2.326E+20	1.45E-11
1200.3	44.19	8.33	2.666E+20	1.58E-11

Table 2

HO_2	
Critical Energy at 0K/kcal $mole^{-1}$	48.10
Frequencies/cm^{-1}	3436, 1392, 1098
Dissociation Energies for Anharmonicities/kcal $mole^{-1}$	50, 65, 100
Product of Adiabatic Moments of Inertia /$10^{60}gm^2\ cm^4$	6.64×10^2
Moment of Inertia: Active External Rotor/$10^{40}gm\ cm^2$	1.365
$H\text{---}O_2$ (Transition State)	
Frequencies	1580
Dissociation Energies for Anharmonicities/kcal $mole^{-1}$	119.2
$I^{\#}/I_{1200}$; $I^{\#}/I_{300}$	1.00; 1.12
Product of Adiabatic Moments of Inertia /$10^{80}gm^2\ cm^4$	(6.64@1200K; 8.32@300K;)$\times 10^2$
Moment of Inertia: Active External Rotor/$10^{40}gm\ cm^2$	6.0@1200K; 9.12@300K
Moment of Inertia: Active 2-D Rotors/$10^{80}gm^2\ cm^4$	0.05(σ=2) [O_2 Moment 24.74 AMU-A^2 Hindered by 99.8%]

Table 3

Collision Partner	β at 300 K	β at 1200 K	β/β_{Ar} at 1200 K	$k_0/k_0(Ar)$ at 1200 K
Ar	0.15	0.056	1	1
N_2	0.31	0.075	3.26	1.76
H_2O	-	0.93	19.8	23.0

References

1. Cobos, C. J., Hippler, H., and Troe, J., *J. Phys. Chem.* 89:342-349 (1985).

2. Pirraglia, A. N., Michael, J. V., Sutherland, J. W. and Klemm, R. B., *J. Phys. Chem.* 93:282-291 (1989).

3. Skinner, G. B., and Ringrose, G. H., *J. Chem. Phys.* 42:2190-2192 (1965).

4. Pamidimukkula, K. M. and Skinner, G. B., *Proceedings Thirteenth Shock Tube Symposium* (C. E. Treanor and J. G. Hall Eds.), SUNY, Albany, 1981, pp. 585-592.

5. Chiang. C.-C. and Skinner, G. B., *Proceedings Twelfth Shock Tube Symposium* (A. Lifshitz and J. Rom Eds.), Magnes Press, Jerusalem, 1980, pp. 629-639.

6. Gutman, D., Hardwidge, E. A., Dougherty, F. A., and Lutz, R. W., *J. Chem. Phys.* 47:4400-4407 (1967).

7. Getzinger, R. W. and Blair, L. S., *Combust. Flame* 13:271-284 (1969).

8. Blair, L. S. and Getzinger, R. W., *Combust. Flame* 14:5-12 (1970).

9. Getzinger, R. W. and Schott, G. L., *J. Chem. Phys.* 43:3237-3247 (1965).

10. Slack, M. W., *Combust. Flame* 28:241-249 (1977).

11. Just, Th. And Schmalz, F., *AGARD Conference Proceedings No. 34, Advanced Components for Turbojet Engines, Part 2*, NATO, Paris, 1968, Paper 19.

12. Dixon-Lewis, G., Greenberg, J. B. and Goldsworthy, F. A., *Sixteenth Symposium (International) on Combustion*, The Combustion Institute, Pittsburgh, PA, 1977, pp. 717-730.

13. Bromly, J. H., Barnes, F. J., Nelson, P. F., and Haynes, B. S., *Int. J. Chem. Kinetics* 27:1165-1178 (1995).

14. Hsu, K.-J., Durant, J. L., and Kaufman, F., *J. Phys. Chem.* 91:1895-1899 (1987).

15. Hsu, K.-J., Anderson, S. M., Durant, J. L., and Kaufman, F., *J. Phys. Chem.* 93:1018-1021 (1989).

16. Carleton, K. L., Kessler, W. J., and Marinelli, W. J., *J. Phys. Chem.* 97:6412-6417 (1993).

17. Davidson, D. F., Petersen, E. L., Röhrig, M., Hanson, R. K., and Bowman, C. T., *Twenty-Sixth Symposium (International) on Combustion*, The Combustion Institute, Pittsburgh, PA, 1996, pp. 481-488.

18. Ashman, P. J. and Haynes, B. S., *Twenty-Seventh Symposium (International) on Combustion*, The Combustion Institute, Pittsburgh, PA, 1998, pp. 185-191.

19. Mueller, M. A., Yetter, R. A., and Dryer, F. L., *Twenty-Seventh Symposium (International) on Combustion*, The Combustion Institute, Pittsburgh, PA, 1998, pp. 177-184.

20. Harding, L. B., Troe, J., and Ushakov, V. G., Phys. Chem. Chem. Phys. 2:631-642 (2000)

21. Davidson, D. F., Bates, R. W., Petersen, E. L., and Hanson, R. K., 35th Aerospace Sciences Meeting & Exhibit, Reno, NV, AIAA 97-0984, (1997).

22. Ashmore, P. G. and Tyler, B. J., *Trans. Farad. Soc.* 58:1108-1116 (1962).

23. Hippler, H., Neunaber, H., and Troe, J., *J. Chem. Phys.*, 103:3510-3516, (1995).

24. Nagali, V., Herbon, J., Horning, D., Bates, R. W., Davidson, D. F., Hanson, R. K., 37th Aerospace Sciences Meeting & Exhibit, Reno, NV, AIAA 99-0942, (1999).

25. Golden, D. M. and Manion, J. A., *Advances in Chemical Kinetics and Dynamics*, JAI Press Inc., Volume 1, pp. 187-276, (1992).

26. Troe, J., *Twenty-Eigth Symposium (International) on Combustion*, The Combustion Institute, PA, 2000, in press.

27. Michael, J. V., *private communication.*